

# PREPARATION OF GRAPHITE PASTE MODIFIED ELECTRODES SUPPORTED BY POLYANILINE AND CHROMIUM OXIDE NANOPARTICLES FOR ELECTROCHEMICAL DETECTION OF UREA

Hanaa Kadhem Egzar<sup>a\*</sup>, Aqeel Mahdi Alduhaidahawi<sup>a</sup>, Sawsan  
D. A. Shubbar<sup>b</sup>, Fadhil Faez Saed<sup>c</sup>

<sup>a</sup>*Department of Chemistry, University of Kufa, Najaf, Iraq*

<sup>b</sup>*Department of Chemical Engineering, University of Kufa, Najaf, Iraq*

<sup>c</sup>*Department of Chemistry, University of Islamic, Najaf, Iraq*

**Abstract:** A graphite paste modified electrodes with Cr<sub>2</sub>O<sub>3</sub> nanoparticles and polyaniline nanocomposite were prepared to study the electrochemical behavior of urea in 1M KOH solution. A co-precipitation simple method was utilized to synthesis the Cr<sub>2</sub>O<sub>3</sub> nanoparticles and chemical polymerization was used to prepare polyaniline (PANI). The modified electrodes under study were prepared by mixing of graphite powder with Cr<sub>2</sub>O<sub>3</sub> nanoparticles and PANI in a ratio of (1/4 w/w). The electrodes were characterized by X-ray diffraction, field emission scanning electron microscopy, cyclic voltammetry and differential pulse voltammetry. The electrocatalytic activity of the electrodes toward urea was investigated. The results indicated that the Cr<sub>2</sub>O<sub>3</sub>/graphite (Cr-G) electrode was more sensitive to urea than PANI /graphite (P-G) or PANI/Cr<sub>2</sub>O<sub>3</sub>/graphite (P-Cr-G) electrodes. The cyclic voltammetry method was used to determine the linear range and limit detection. Accordingly, the modified electrode (Cr-G) showed a linear range of (0.001 - 0.040) mM and a detection limit was 0.00637 mM. Moreover, the kinetic characteristics of urea, like transfer coefficient and the rate constant, were examined in an alkaline media.

**Keywords:** Polyaniline, Chromium oxide nanoparticales, Modified electrode, Cyclic voltammetry, Detection limit of urea.

---

\* Hanaa, Egzar, *e-mail:* hanaak.abdullah@uokufa.edu.iq

## Introduction

Urea is an organic compound produced in industry on a large scale as animal feed additives and as agricultural fertilizers. Large amounts of domestic effluents and wastewater containing urea are generated from human and animal urine; an adult produces about 33 g of urea per day, this results in high concentration of urea in wastewater. Wastewater containing urea causes several environmental problems, because of the natural decomposition of urea to ammonia. The emission of ammonia that produced from decomposition of urea in the atmosphere may oxidize in the atmosphere to nitrogen oxides, forming nitrogen pollutants, such as, nitrates, nitric oxides, nitrites, and may promote the formation of acid rain<sup>1</sup>. Therefore, detecting, removing urea from wastewater and reducing its impact on the environment has become a focus of interest for many researchers. At present, many methods are used to detect urea, including gas chromatography, high-performance liquid chromatography, fluorescence method, capillary electrophoresis, electrochemical method, enzyme method, and spectrophotometry measurement.<sup>2</sup> Many studies have suggested that electrochemical methods are among the most commonly used methods for the detection of urea due to their high sensitivity, stability, high selectivity, simplicity, and low cost.<sup>3</sup>

Electrochemical methods involve utilizing several types of chemically modified electrodes (CMEs) that have wide chemical applications such as sensing and biosensing, energy storage (capacitors and batteries).<sup>4</sup> Utilizing CME can enhance the charge transfer kinetics with low overpotential, increase the sensitivity by expanding the surface area, surface activity and accessible reactive sites and improve the selectivity of

the analytes in the presence of interferences, reduces fouling and enhances chemical and electrochemical stability.<sup>5</sup>

Carbon paste electrode (CPE) is an example of the most widely used chemical electrodes, due to its important properties, such as very high melting point, insolubility in water and good electrical conductivity,<sup>6</sup> the repeatable surface area, simplicity of preparation, and low residual current in potentially large windows.<sup>7</sup> However, this electrode has several disadvantages, such as lower stability when working in a wide range of potentials, slower speed of electron transfer, lower sensitivity and reproducibility. A typical and a suitable method to overcome advantages of CPE is the chemical modification of it, which leads to the construction of new sensors with desirable quantitative properties.<sup>8</sup> The modification of the CPE size gives a renewed electrode surface for each measurement and this reduces the determination error by the adsorption of the analyte on the surface of the electrode.<sup>9</sup>

Recently, polymer modified electrodes (PMEs) have received a great attention due to their reproducibility, good stability, active sites, strong adhesion to the electrode surface and homogeneity in electrochemical deposition. In many cases, the signals increase by several orders of magnitude in the conjugated polymer-modified working electrode when compared to the unmodified electrode.<sup>10,11</sup> Common polymers that used in electrodes are polyaniline and its derivatives, chitosan, polypyrrole, polyacetylene, polythiophene and its derivatives. The benefits of using polyaniline in sensors field are specified by signal amplification, selectivity, sensitivity of the analyte, and elimination of contamination.<sup>12,13</sup>

Electrode modification with nanoscale oxides is an attractive methodology for improving the area and potential of used electrodes.<sup>14</sup>

Nanoscale metal oxides have received great interest in the field of sensors applications, because of their characteristics, such as simplicity of fabrication, possibility of controlling crystal shape and size, optical and catalytic properties, chemical compatibility, electron transfer kinetics, and adsorption capacity.<sup>15</sup>

Since a long time, Carbon paste electrode modified using different modifiers were broadly utilized in the analysis of many analytes.<sup>16-19</sup> Between them various of the fabricated sensors applied for the analysis of urea are, Ni(II)-clinoptilolite nanoparticles<sup>20</sup> polymeric particles (urethane-urea) containing urease,<sup>21</sup> Hybrid ZnO nanostructures modified graphite electrode,<sup>22</sup> PANI/graphite,<sup>23</sup> etc.

In this work, polyaniline and chromium oxide nanoparticles were prepared by simple methods. The PANI and Cr<sub>2</sub>O<sub>3</sub> were then used for the modification of graphite paste electrodes (P-G), (Cr-G) and (P-Cr-G). The modified electrodes were lastly utilized as a working electrode in three electrodes electrochemical cell for electro-oxidation of urea in alkaline media. The transfer coefficient and the rate constant at Cr-G electrode was evaluated by Laviron's equation. The electrocatalytic activity of electrodes toward urea detection was investigated by cyclic voltammetry (CV) and differential pulse voltammetry (DPV).

## Results and Discussion

### *Characterization of composite material by X-ray diffraction*

The new modified electrodes are characterized by X-ray diffraction studies. XRD patterns of graphite, polyaniline and chromium oxide nanocomposites are shown in Figure 1. When comparing the X-ray diffraction pattern of pure graphite with chromium oxide (Cr<sub>2</sub>O<sub>3</sub>), polyaniline (PANI), Cr<sub>2</sub>O<sub>3</sub>/PANI loaded graphite, it was found that all

spectra contain peaks  $25.3^\circ$ ,  $33.3^\circ$ ,  $53.5^\circ$  and  $76.4^\circ$  with a slight shift about of  $0.03^\circ$ ,  $0.6^\circ$ , and  $0.03^\circ$ , respectively. The peak  $25.3^\circ$  belongs to the micro-crystallinity structure of graphite,<sup>24</sup> as crystalline graphite shows a peak at  $26.6^\circ$ . A decrease in the intensity of the peak  $25.3^\circ$  was observed from 7950 to 2401, 4090 and 1669 in the case of mixing chromium oxide, aniline and a mixture of chromium oxide and aniline with graphite, respectively, which confirms the occurrence of an interaction between the graphite and the loading materials. XRD patterns of the Cr-G nanocomposite show a trigonal poly-crystalline structure of  $\text{Cr}_2\text{O}_3$  (criterion card No. 96-900-0047) emerged with peaks indexed at (202) at  $32.4^\circ$ , (242) at  $48.9^\circ$  and (602) at  $69.1^\circ$  (Figure 1B).<sup>25</sup>

The patterns of XRD of P-G electrode demonstrate the peaks (010) at  $19.7^\circ$  and (310) at  $28.6^\circ$  Figure 1C; that corresponded to a semicrystalline nature of polyaniline in emeraldine form.

The mean particle size for synthesized composites Cr-G, P-G and P-Cr-G was 19 nm, 18 nm and 17 nm respectively, that were calculated by the application of well-defined Scherrer's Equation (1).<sup>26</sup>

$$D = \frac{K\lambda}{\beta \cos \theta} \quad (1)$$

D, is the crystal size;  $\lambda$ , is the wavelength ( $1.54059 \text{ \AA}$ ) of the X-rays; K, is the shape factor (0.94);  $\theta$ , is the diffraction angle and  $\beta$ , is the full width at half maximum (FWHM) of the diffraction peaks.

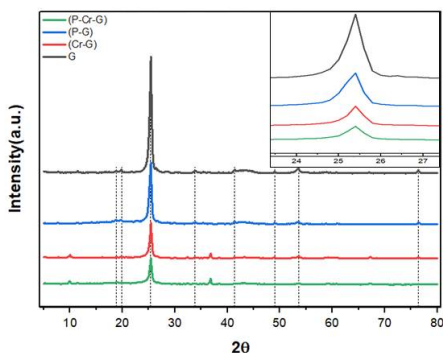


**Figure 1.** Typical XRD patterns of graphite G and modified graphite electrodes Cr-G electrode, P-G electrode and P-Cr-G electrode.

### *Characterization of composite material by Field Emission Scanning Electron Microscopy*

The modified graphite electrodes were characterized by field emission - scanning electron microscopy (FE-SEM). The results of FE-SEM show the shape and the size of nanocomposites, and also, show the morphology and size of chromium oxide particles distributed on the surface of graphite with irregular spherical shape and irregular size (Figure 2a-c). The electrocatalytic effectiveness of Cr-G electrode, is attributed to the surface roughness and structure defects.

On the other hand, Figure 2d-f shows the shape and the size of polyaniline, with a regular distribution of polymer particles around the graphite, which has slightly irregular rod and spherical structure with a size of approximately 21 nm.

Figure 2g-i shows the morphology of composite that resulted from mixing polyaniline and chromium oxide with graphite. We noticed the presence of rod structures of the polymer and irregular spherical particles of oxide on the surface of graphite with a size of 30 nm.

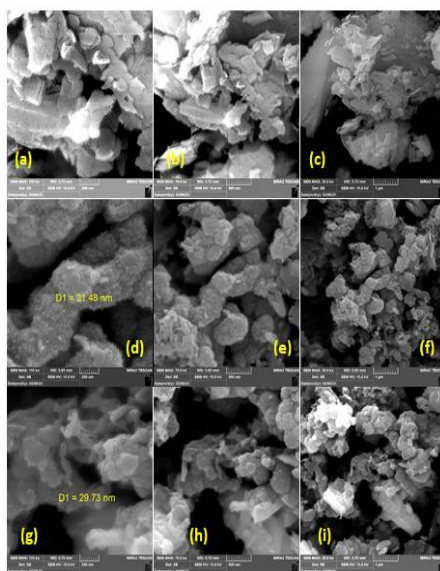


**Figure 2.** FE-SEM images of: (a-c) chromium oxide, (d-f) polyaniline, (g-i) polyaniline-chromium oxide modified graphite electrodes.

*Electrocatalytic detection of urea at different modified electrodes*

The electrochemical behavior of different graphite modified electrodes towards the detection of urea was identified by CV technique in a solution of 0.02 mM urea and 1M KOH. Cyclic voltammogram of graphite modified with  $\text{Cr}_2\text{O}_3$  (Cr-G), polyaniline (P-G) and  $\text{Cr}_2\text{O}_3$ / polyaniline (P-Cr-G) in 0.02 mM urea /1 M KOH are displayed in Figure 3. It is shown that Cr-G electrode has high electrocatalytic activity towards urea detection (Figure 3B) compared to P-G or P-Cr-G due to large surface area and porous nature of chromium oxide which increased the efficiency of Cr-G towards urea oxidation. Although, P-G has well electrocatalytic activity to urea oxidation (Figure 3A) this may be attributed to the good conductivity of polyaniline. P-Cr-G composite has no electroactivity towards urea detection (Figure 3C).

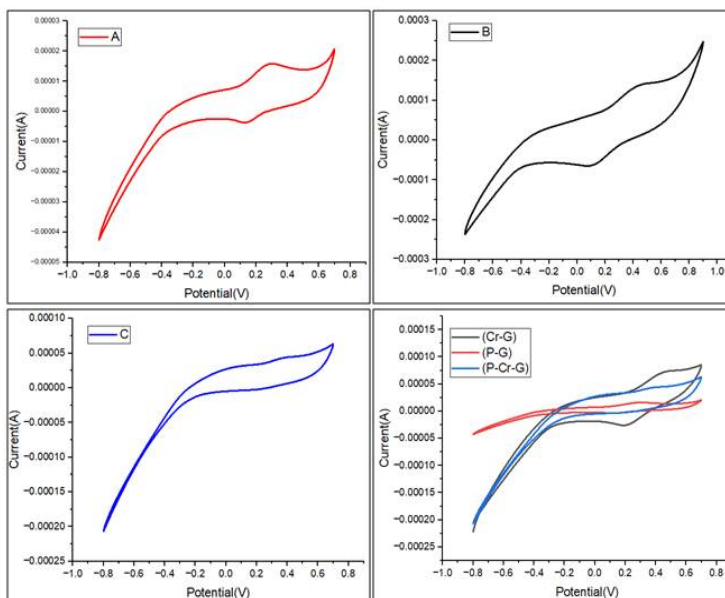


**Figure 3.** CVs of: (A) P-G electrode, (B) Cr-G electrode and (C) P-Cr-G electrode, (D), CVs of (Cr-G, P-G and P-Cr-G) electrodes, were obtained in the presence of urea (0.02 mM) in (1M) of KOH at a scan rate of  $20 \text{ mVs}^{-1}$ .

Figure 3 shows a pair of redox peaks centered at 0.151/0.355V that are well defined for the reversible oxidation–reduction pair (Cr(III)/Cr(VI)) in the case of the modified Cr-G electrode, which indicates the presence of an electrically active center for redox reactions that represented by the equation below:



In the alkaline medium, urea was adsorbed on  $\text{CrO}(\text{OH})_2$  and direct oxidation of urea was taking place. Furthermore,  $\text{CrO}(\text{OH})_2$  was reduced to  $\text{Cr}(\text{OH})_3$  at the time of urea oxidation. A pair of redox peaks at 0.129V/0.305 V is observed in the case of using a modified P-G electrode (Figure 3B), which is attributed to the redox process that normally occurred for the polyaniline system. As shown in (Figure 3C), there was no observable redox peak for P-Cr-G modified electrode due to its redox inactivity, however, the polyaniline/chromium oxide (PANI/  $\text{Cr}_2\text{O}_3$ ) composite showed a larger area (Figure 3C), indicating the composite has a higher capacitance than PANI, due to the incorporation and synergistic interactions between PANI and  $\text{Cr}_2\text{O}_3$ .

As a result of Cr-G electrode performance which exhibited an excellent current response toward urea, it was used for urea detection in all the experiments in this work.

#### *Influence of scan rate*

The influence of scan rate on the response of 0.02 mM of urea was investigated with graphite-  $\text{Cr}_2\text{O}_3$ (Cr-G) modified electrode in 1 M KOH within the range of scan rate (10-200 mV) (Figure 4). It is viewed the increase of the anodic and cathodic peaks current density with increased of scanrate which pointing at electro chemical oxidation of urea on (Cr-G) electrode is a diffusion controlled process. The  $E_{\text{cathodic}}$  peak potential shifted to a more negative potential, while the anodic peaks shifted in the

opposite direction, this is as a result of the rise in the electrode resistance in height scan rates.<sup>27</sup>

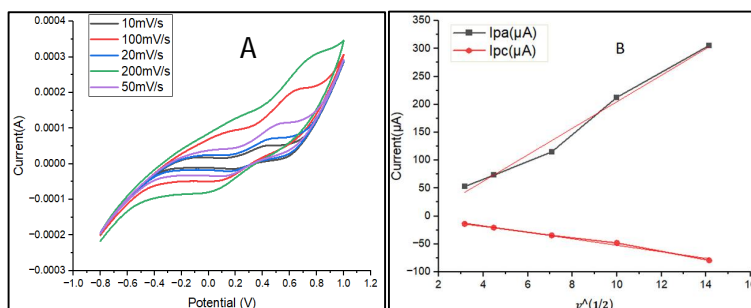


**Figure 4.** (A) CVs of Cr-G in 0.02 mM urea and 1M KOH at scan rate 50 mV/s. (B) Relation between the cathodic and anodic peaks currents of urea solution with square root of scan rate.

Figure 4B shows the relationship between the anodic and cathodic current values with the square root of the scan rate. The anodic and cathodic peak current increased linearly with scan rate in conformity with the equations:

$$I_{pa} (\mu A) = 23.748 v^{1/2} - 32.644 (R^2 = 0.9868)$$

and

$$I_{pc} (\mu A) = -5.8219 v^{1/2} + 5.8376 (R^2 = 0.9896).$$

This means that the electrochemical process is restricted by the diffusion rate of urea from the solution to the surface of the working electrode.<sup>28</sup>

The plot of the logarithm peaks current (cathodic and anodic) vs the logarithm of scan rate is shown in Figure 5A, which is conformed with the equations:

$$\log I_{pa} (\mu A) = 0.6003 \log v + 1.0956 (R^2 = 0.9875)$$

$$\log I_{pc} (\mu A) = -0.5651 \log v - 0.5794 (R^2 = 0.9969).$$

The slopes of anodic and cathodic peaks currents were 0.6003 and 0.5651 respectively, the slopes values is between 0.5 and 1, indicating that

demonstrates the diffusion and adsorption are the common controlled process.<sup>29</sup>

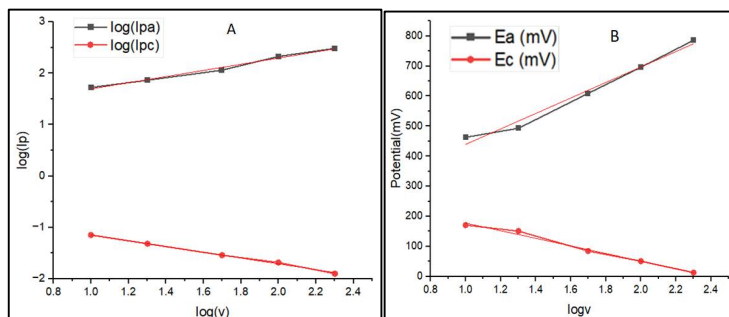


**Figure 5.** (A) Relation between log of redox peaks current and log of scan rate, (B) relation between peaks potential and log of scan rate of urea oxidation.

Figure 5B shows the dependence of peak potential on logarithm of scan rate and the equations that corresponded to their relationship are illustrated in the equations:

$$E_a \text{ (mV)} = 257.25 \text{ Log } v + 182.32 \quad (R^2 = 0.9814) \quad (2)$$

$$E_c \text{ (mV)} = -126.48 \text{ Log } v + 304.18 \quad (R^2 = 0.9891) \quad (3)$$

According to Laviron equation<sup>30</sup>:

$$E_p = E_0 + \frac{RT}{\alpha nF} - \frac{RT}{\alpha nF} \ln v \quad (4)$$

where  $n$  is the number of electron,  $\alpha$  is the cathodic electron transfer coefficient,  $R = 8.314 \text{ J/mol.K}$ ,  $F = 96500 \text{ C/mol}$  and  $T = 298 \text{ K}$ . A graph of  $E_p = f(\log v)$  Figure 5B gives two straight lines with a slope equal to  $(\frac{-2.3RT}{\alpha nF})$  and  $(\frac{2.3RT}{(1-\alpha)nF})$  for cathodic and anodic peaks respectively. From slopes of  $E_p$  versus  $\log v$  the cathodic transfer coefficient was calculated to be 0.467 (given  $0.3 < \alpha n < 0.7$ ) in general,<sup>31</sup> then the number of electrons  $n = 1$ , that means one electron was transferred in the electrochemical redox reaction of urea. In order to calculate the value of apparent heterogeneous electron transfer rate constant ( $k_s$ ), the following Laviron equation was used:

$$\log k_s = \alpha \log(1 - \alpha) + (1 - \alpha) \log \alpha - \log \frac{RT}{nFv} - \frac{\alpha(1-\alpha)\Delta E_p nF}{2.303RT} \quad (5)$$

$\Delta E_p$  is the separation of the redox peaks (0.292V),  $v$  is the scan rate (0.01V),  $k_s$  was calculated to be  $0.0114 \text{ s}^{-1}$ .

#### Effect of urea concentrations

Figure 6A shows cyclic voltammetric response of the electrocatalytic oxidation of urea at different concentrations (0.0025, 0.005, 0.01, 0.02, 0.025, 0.03, 0.035, 0.04) mM by using Cr-G as working electrode in 1 M KOH. It was noted that the cathodic and anodic peak currents raised with increasing urea concentration, and the peak separation  $\Delta E_p$  remained constant, approximately 240 mV. The increasing in the anodic and cathodic peak current with increase of urea concentrations refer to the electrooxidation of urea and indicated the electrocatalytic behavior of Cr-G electrode.

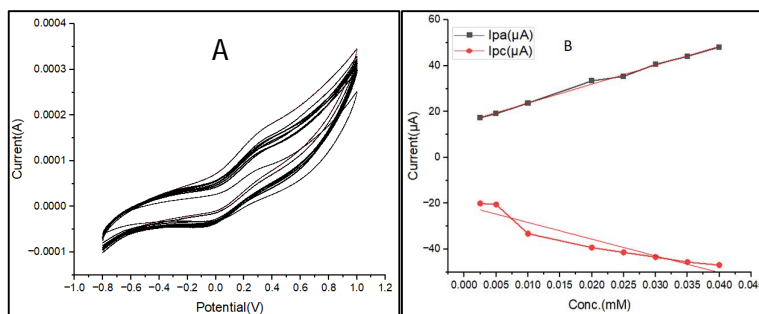


**Figure 6.** (A) Effect of urea concentration on CV response of urea in 1M KOH with scan rate of  $50 \text{ mVs}^{-1}$  on Cr-G modified electrode. (B) plot of anodic peaks current vs concentrations of urea.

A plot of the cathodic and anodic peaks current vs. urea concentrations is shown in Figure 6B. The standard deviation ( $s_{dyx}$ ), the limit of detection (LOD), correlation coefficient ( $R^2$ ), and limit of quantification (LOQ) of the cathodic and anodic peaks current were calculated by equation (6) and equation (7)<sup>32,33</sup> and illustrated in table 1.

$$\text{LOD} = \frac{3 \times s_{dyx}}{m} \quad (6)$$

$$\text{LOQ} = \frac{10 \times s_{dxy}}{m} \quad (7)$$

where (m) represents the slope of the calibration curve, and (sdyx) is the standard deviation of the anodic peaks current.

**Table 1.** Detection parameters at Graphite-Cr<sub>2</sub>O<sub>3</sub> (Cr-G) modified electrode for the concentration series of 0.025 to 0.040 mM.

Parameter	Anodic peak current	Cathodic peak current
R <sup>2</sup>	0.98065	0.9018
sdyx	1.13259	3.637274
LOD	0.02126mM	0.049936 mM
LOQ	0.00637 mM	0.049936 mM

### Differential Pulse Voltammetric Investigation(DPV)

The electrochemical performances of different prepared electrodes (P-G, Cr-G and P-Cr-G) were determined using differential voltammetry (DPV) measurements to assess the electrochemical sensitivity of Cr-G for urea detection.

As shown in figure 7, the peak current of (P-G) electrode is 18.96  $\mu$ A for urea. When the (Cr-G) electrode was used, the peak current of urea increased to 33.36  $\mu$ A, which can be attributed to the interaction between urea and Cr<sub>2</sub>O<sub>3</sub> NPs. The peak current of (P-Cr-G) was 0.02757  $\mu$ A, which means that composite did not cause significant changes in the peak current for urea and these results are identical to the results of previously measured cyclic voltammetry.

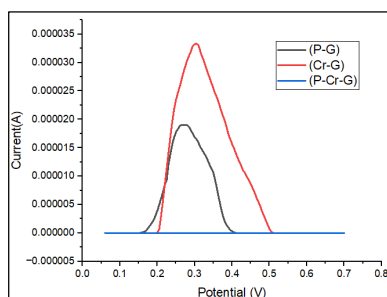


**Figure 7.** Differential pulse voltammogram recorded for a urea in 1 M KOH solution at (P-G),(Cr-G) and (P-Cr-G) electrodes.

---

## Experimental

### *Materials*

Chromium sulfate  $\text{Cr}_2(\text{SO}_4)_3$ , ammonium hydroxide (liquor ammonia), polyvinylpyrrolidone (PVP), lithium chloride (LiCl), hydrochloric acid (HCl), aniline ( $\text{C}_6\text{H}_5\text{NH}_2$ ), ammonium persulfate ( $(\text{NH}_4)_2\text{S}_2\text{O}_8$ ), urea  $\text{CO}(\text{NH}_2)_2$  and potassium hydroxide (KOH) were purchased from Sigma Aldrich and were used as received.

### *Synthesis of chromium oxide nanoparticles*

Aqueous ammonia was added dropwise with continuous stirring to (100 mL) of (0.1 M)  $\text{Cr}_2(\text{SO}_4)_3$  solution containing (2.0 g) of PVP. The precipitate was filtered and washed with ethanol and then with deionized water several times. The precipitate was dried at  $70^\circ\text{C}$  for 48 h. The precipitate was calcined at  $600^\circ\text{C}$  for 5h.<sup>34</sup>

### *Chemical polymerization of aniline*

Lithium chloride (20.8 g) was dissolved in 1 M of hydrochloric acid (125 mL), aniline (5.0 g) was dissolved in 75 mL of HCl/LiCl solution and cooled to  $-3^\circ\text{C}$  (by low temperature thermostat cooling circulation) and ammonium persulfate (12.3g) was also dissolved in 50 mL of the remaining solution of HCl/LiCl and cooled to  $-3^\circ\text{C}$ . The two solutions were mixed together at a constant temperature ( $-3^\circ\text{C}$ ) for 3 h, the product was filtered, and the precipitate was washed with distilled water several times and then dried.<sup>35</sup>

### *Preparation of modified electrodes*

The modified graphite paste electrodes were prepared by mixing polyaniline with graphite powder in a ratio of (1/4w/w) in 10 mL of ethanol

at 35°C for 3 h with continuous stirring, and then the material was dried with hot air for 8 h. The same method was used to prepare graphite paste modified with chromium oxide nanoparticles, as well as polyaniline and chromium oxide composites. To obtain sufficient and homogeneous graphite paste the mixture of graphite and solid paraffin wax was mixed in a ratio of 7/3 in an agate slurry. The composite material was packed in a glass tube (2.5 mm in diameter). To ensure electrical contact, a copper wire was inserted from the open side of the tube into the dough.

### *Electrochemical experiments*

Cyclic voltammetry (CV) measurement was achieved by using a DY2000 series Potentiostat. Each system was controlled by a computer and the software packages that used were Windows 8/7/XP only. Three standard (100mL) electrochemical cells consisting of a platinum wire were used as a counter electrode and a reference electrode (Ag/AgCl) for referred potential.

### **Conclusions**

Chromium oxide ( $\text{Cr}_2\text{O}_3$ ) nanoparticles and polyaniline were prepared. Then, the graphite paste was modified with chromium oxide, polyaniline, and a mixture of polyaniline and chromium oxide which were applied to determine the urea using CV and DPV techniques. Due to the porous structure and large surface area, the graphene electrode modified with  $\text{Cr}_2\text{O}_3$  NPs showed good electrochemical performance toward urea, showing a wide linear range and low detection limit. Moreover, the results indicated good sensitivity for the graphite electrode modified with polyaniline, but when mixing the graphite paste with a mixture of chromium oxide and polyaniline, it did not give electrocatalytic activity toward urea.

Due to the high sensitivity of the graphite /Cr<sub>2</sub>O<sub>3</sub> NPs modified electrode, it can be successfully used to study the electrochemical behavior of urea.

### Acknowledgements

We appreciate the help of the laboratory staff at the Department of Chemistry, Faculty of Science, Kufa University, Najaf, Iraq.

### References

1. Asran, A.; Mohamed, M. A.; Ahmed, N.; Banks, C. E.; Allam, N. K. An innovative electrochemical platform for the sensitive determination of the hepatitis B inhibitor Entecavir with ionic liquid as a mediator. *J. Mol. Liq.* **2020**, *302*, 112498.
2. He, C.; Hou, L.; Wang, Y. Electrochemical behavior of uric acid at a glassy carbon electrode modified with poly-ninhydrin derivative. *Rev. Roum. Chim.* **2022**, *67*, 207–216.
3. Yao, D.; He, Z.; Wen, G.; Liang, A.; Jiang, Z. A facile and highly sensitive resonance Rayleigh scattering-energy transfer method for urea using a fullerene probe. *RSC Adv.* **2018**, *8*, 29008–29012.
4. Kailasa, S.; Rani, B.; Reddy, M. S.; Jayarambabu, N.; Munindra, P.; Sharma, S. K.; Rao, K. V. NiO nanoparticles-decorated conductive polyaniline nanosheets for amperometric glucose biosensor. *Mater.Chem.Phys.* **2019**, *242*, 122524.
5. Ciucu, A. A. Chemically Modified Electrodes in Biosensing. *J. Biosens. Bioelectron.* **2014**, *5(3)*, 1000154.
6. Chen, T. W.; Yu, X. N.; Li, S. J. Simultaneous Determination of Dihydroxybenzene Isomers using Glass Carbon Electrode Modified with 3D CNT-graphene Decorated with Au Nanoparticles. *Int. J. Electrochem. Sci.* **2019**, *19*, 7037–7046.
7. Sawkar, R. R.; Shanbhag, M. M.; Tuwar, S. M.; Veerapur, R.S.; Shetti, N. P. Glucose Incorporated Graphite Matrix for Electroanalysis of Trimethoprim. *Biosensors* **2022**, *12*, 909.
8. Mehmeti, E.; Stanković, D.M.; Chaiyo, S.; Švorc, L.; Kalcher, K. Manganese dioxide-modified carbon paste electrode for voltammetric determination of riboflavin. *Microchim. Acta* **2016**, *183*, 1619–1624.
9. Tajik, S.; Beitollahi, H.; Nejad, F. G.; Safaei, M.; Zhang, K.; Le, Q. V.; Varma, R. S.; Jang, H. W.; Shokouhimehr, M. Developments and applications of

- nanomaterial-based graphite paste electrodes. *RSC Adv.* **2020**, *76*, 21561–21581.
10. Vural, K.; Karakaya, S.; Dilgin, D.; Gökçel, H.; Dilgin, Y. Voltammetric determination of Molnupiravir used in treatment of the COVID-19 at magnetite nanoparticle modified carbon paste electrode. *Microchem. J.* **2023**, *6*, 108195.
  11. Dulgerbaki, C.; Oksuz, A.U. Fabricating polypyrrole/tungsten oxide hybrid based electrochromic devices using different ionic liquids. *Polym. Adv. Technol.* **2016**, *15*, 73–81.
  12. Massoumi, B.; Davtalab, S.; Jaymand, M.; Entezamic, A.A. AB<sub>2</sub> Y-shaped miktoarm star conductive polyaniline-modified poly(ethylene glycol) and its electrospun nanofiber blend with poly(3-caprolactone). *RSC Adv.* **2015**, *34*, 36715–36726.
  13. El-Beshlawy, M. M.; Abdel-Haleem, F. M.; Kamel, A. H.; Barhoum, A. Screen-Printed Sensors Coated with Polyaniline/Molecularly Imprinted Polymer Membranes for the Potentiometric Determination of 2,4-Dichlorophenoxyacetic Acid Herbicide in Wastewater and Agricultural Soil. *Chemosensors* **2023**, *11*, 3.
  14. Kulikova, T.; Porfireva, A.; Evtugyn, G.; Hianik, T. Electrochemical DNA Sensors with Layered Polyaniline–DNA Coating for Detection of Specific DNA Interactions. *Sensors* **2019**, *19*(3), 469.
  15. Radhi, M. M.; Mossa, A. A.; Al-Mulla, E. A. J.; Lafta, A.N. Electrochemical Study of Modified Glassy Carbon Electrode with Polyaniline Nanoparticles Using Cyclic Voltammetry. *Bull. Chem. Soc. Ethiop.* **2022**, *36*, 687–696.
  16. Rajendrachari, S. Carbon composite voltammetric sensors for food quality assessment. *Materials* **2022**, *8*, 8–13.
  17. Chandrashekar, B. N.; Kumara Swamy, B. E.; Pandurangachar, M.; Sharat Shankar, S.; Gilbert, O.; Manjunatha, J. G.; Sherigara, B. S. Electrochemical oxidation of dopamine at polyethylene glycol modified carbon paste electrode: A cyclic voltammetric study. *Int. J. Electrochem. Sci.* **2010**, *5*, 578–592.
  18. Patil, V. B.; Ilager, D.; Tuwar, S. M.; Mondal, K.; Shetti, N. P. Nanostructured ZnO-Based Electrochemical Sensor with Anionic Surfactant for the Electroanalysis of Trimethoprim. *Bioengineering* **2022**, *9*, 521.
  19. Sawkar, R. R.; Shanbhag, M. M.; Tuwar, S. M.; Mondal, K.; Shetti, N. P. Sodium Dodecyl Sulfate-Mediated Graphene Sensor for Electrochemical Detection of the Antibiotic Drug: Ciprofloxacin. *Materials* **2022**, *15* 7872.
  20. Ahmadi, A.; Nezamzadeh-Ejhi, A. A comprehensive study on electrocatalytic current of urea oxidation by modified carbon paste electrode

- with Ni(II)-clinoptilolite nanoparticles: Experimental design by response surface methodology. *J. Electroanal. Chem.* **2017**, *801*, 328–337.
21. Razumiene, J.; Sakinyte, L.; Kochane, T.; Maciulyte, S.; Straksys, A.; Budriene, S.; Barkauskas, J. Carbon Electrode based Urea Sensor Modification of Graphite and New Polymeric Carriers for Enzyme Immobilization. *Biodevices* **2013**, 197–201.
  22. Dhinasekaran, D.; Soundharraj, P.; Jagannathan, M.; Rajendran, A. R.; Rajendran, S. Hybrid ZnO nanostructures modified graphite electrode as an efficient urea sensor for environmental pollution monitoring. *Chemosphere* **2022**, *296*, 133918.
  23. Das, D.; Das, J.; Deb, K.; Chakraborty, S.; Saha, B. A low-cost flexible material system made of PANI/graphite for resistive detection and quantitative determination of urea. *Mater. Chem. Phys.* **2023**, *301*, 127573.
  24. Wang, H.; Han, W.; Li, X.; Liu, B.; Tang, H.; Li, Y. Solution Combustion Synthesis of Cr<sub>2</sub>O<sub>3</sub> Nanoparticles and the Catalytic Performance for Dehydrofluorination of 1,1,1,3,3-Pentafluoropropane to 1,3,3,3-Tetrafluoropropene. *Molecules* **2019**, *24*, 361.
  25. Abdullah, S. H.; Humud, H. R.; Mustafa, F. I. A Single Layer of Chromium Oxide Nanoparticles Films Coated with Graphite by Applying Exploding Wire Technique for Efficient Solar Selective Absorber. *Iraqi J. Sci.* **2022**, *63*, 4273–4281.
  26. Aladeemy, S. A.; Al-Mayouf, A. M.; Amer, M. S.; Alotaibi, N.H.; Wellerc, M. T.; Ghanem, M. A. Structure and electrochemical activity of nickel aluminium fluoride nanosheets during urea electro-oxidation in an alkaline solution. *RSC Adv.* **2021**, *11*, 3190–3201.
  27. Ghaedamini, H.; Duanghathaipornasuk, S.; Onusko, P.; Binsheheween, A. M.; Kim, D. S. Reduced Glutathione-Modified Electrode for the Detection of Hydroxyl Free Radicals. *Biosensors* **2023**, *13*, 254.
  28. Lang, J.; Wang, W.; Zhou, Y.; Guo, D.; Shi, R.; Zhou, N. Electrochemical Behavior and Direct Quantitative Determination of Paclitaxel. *Front. Chem.* **2022**, *10*, 1–9.
  29. Saisahas, K.; Soleh, A.; Promsuwan, K.; Saichanapan, J.; Phonchai, A.; Mohamed Sadiq, N. S.; Teoh, W. K.; Chang, K. H.; Lim Abdullah, A. F.; Limbut, W. Nanocoral-like Polyaniline-Modified Graphene-Based Electrochemical Paper-Based Analytical Device for a Portable Electrochemical Sensor for Xylazine Detection. *ACS Omega.* **2022**, *7*, 13913–13924.
  30. Lu, Y.; Wang, Z.; Mu, X.; Liu, Y.; Shi, Z.; Zheng, Y.; Huang, W. The electrochemical sensor based on Cu/Co binuclear MOFs and PVP cross-linked derivative materials for the sensitive detection of luteolin and rutin. *Microchem. J.* **2022**, *175*, 107131.
  31. Thomas, D.; Rasheed, Z.; Jagan, J. S.; Kumar, K. G. Study of kinetic parameters and development of a voltammetric sensor for the determination of

- butylated hydroxyanisole (BHA) in oil samples. *J. Food Sci. Technol.* **2015**, *52*, 6719–6726.
32. Rageh, H. M.; Abou-Krishna, M. M.; Abo-bakr, A.M.; Abd-Elsabour, M. Electrochemical Behavior and the Detection Limit of Ascorbic Acid on a Pt Modified Electrode. *Int. J. Electrochem. Sci.* **2015**, *10*, 4105-4115.
  33. Elugoke, S. E.; Fayemi, O. E.; Adekunle, A. S.; Sherif, E. M.; Ebenso, E. E. Electrochemical sensor for the detection of adrenaline at poly(crystal violet) modified electrode: optimization and voltammetric studies. *Heliyon* **2022**, *10*, 1-28.
  34. Mohammed, F. H.; Mikhlif, H. M. Optical, Structural, Morphological Properties of Chromium (III) Oxide Nanostructure Synthesized Using Spray Pyrolysis Technique. *Iraqi J. Phys.* **2021**, *19*, 79–86.
  35. Singha, B.; Dasa, B. Synthesis and characterization of crystalline polyaniline. *Indian J. Pure Appl. Phys.* **2020**, *58*, 735–739.